metals

Article

The Effect of Mean Load for S355J0 Steel with Increased Strength

Roland Pawliczek * and Dariusz Rozumek

Department of Mechanics and Machine Design, Opole University of Technology, Mikolajczyka 5, 45-271 Opole, Poland; d.rozumek@po.edu.pl

* Correspondence: r.pawliczek@po.edu.pl; Tel.: +48774498404

Received: 12 December 2019; Accepted: 28 January 2020; Published: 1 February 2020

Abstract: The paper presents an algorithm for calculating the fatigue life of S355J0 steel specimens subjected to cyclic bending, cyclic torsion, and a combination of bending and torsion using mean stress values. The method of transforming cycle amplitudes with a non-zero mean value into fatigue equivalent cycles with increased amplitude and zero mean value was used. Commonly known and used transformation dependencies were used and a new model of the impact of the mean stress value on the fatigue life of the material was proposed. The life calculated based on the proposed algorithm was compared with the experimental life. It has been shown that the proposed model finds the widest application in the load cases studied, giving good compliance of the calculation results with the experimental results.

Keywords: fatigue life; steel; bending and torsion; stress ratio

1. Introduction

Algorithms for calculating fatigue life are built from a series of steps that determine how to perform calculations to take into account many factors describing the load parameters of an element. Numerous papers present the results of fatigue tests describing the behavior of the material and experimental verification of the proposed models [1–8]. In the case of fatigue tests during bending and torsion with the participation of the mean load value, such an algorithm is widely presented in [6,9–11] and allows determining the fatigue life of tested specimens under various load conditions. The results of such analyzes require accurate knowledge of the behavior of the tested material under various loading conditions. It is necessary to have a wide spectrum of results of fatigue tests conducted in different conditions, which take into account the influence of the average load value and different specimen geometry [9–11]. Such tests are designed to understand the properties of the material and allow verification of the proposed calculation algorithms in terms of compliance with the results of the experiment. Kluger and Pawliczek [6] shows and discusses on the results of a comparison involving mathematical models applied for fatigue life calculations where the mean load value is taken into account. The specimens were subjected to bending, torsion and a combination of bending with torsion with mean value of the load. Analysis of the calculation results show that the best fatigue life estimations are obtained by using models that are sensitive to the changes of material behavior under fatigue loading in relation to the specified number of cycles of the load. Branco et al. [9] described studies the effect of different loading orientations on fatigue behavior in severely notched round bars under pulsating in-phase combined bending-torsion loading. Fatigue life is predicted via the Coffin-Manson model. The paper [11] presents results on the fatigue crack in specimens made of the 2017A-T4 alloy under bending. The specimens had different notch geometry. The tests were performed by imposing a constant load amplitude value and different stress ratio $R = -1.0$ and $R = 0$. In [12] the failure analysis of a coupled shaft from a shredder is presented, which was subjected to bending and torsion. The shaft failure occurred due to fatigue, on a perpendicular plane to the rotation axis, in the place of the hole. The shaft fracture surface presents characteristics of fatigue due to torsion combined with bending high loads.

The purpose of the tests described in the work is to learn about the behavior of specimens made of typical structural steel under conditions of cyclic loads with different stress ratios. An approach consisting of the reduction of the multiaxial (complex) load state to a simple load state (uniaxial tension-compression) and prediction of fatigue life of elements using the linear Palmgren-Miner damage hypothesis is presented. The results of calculations based on fatigue characteristics at uniaxial tensile-compression are compared with the results of experimental tests of S355J0 steel specimens subjected to cyclic bending, cyclic torsion and a combination of bending and torsion using non-zero mean stress values.

2. Analyzed Fatigue Models

The models described below relate to stress amplitude change σ_a (τ_a) and mean stress value σ_m (τ_m). Figure 1 shows the algorithm for calculating fatigue life under bending and torsion for courses with different values of the stress ratio R. In the algorithm, the equivalent stress amplitude was calculated using the Huber–Misess–Hencky hypothesis.

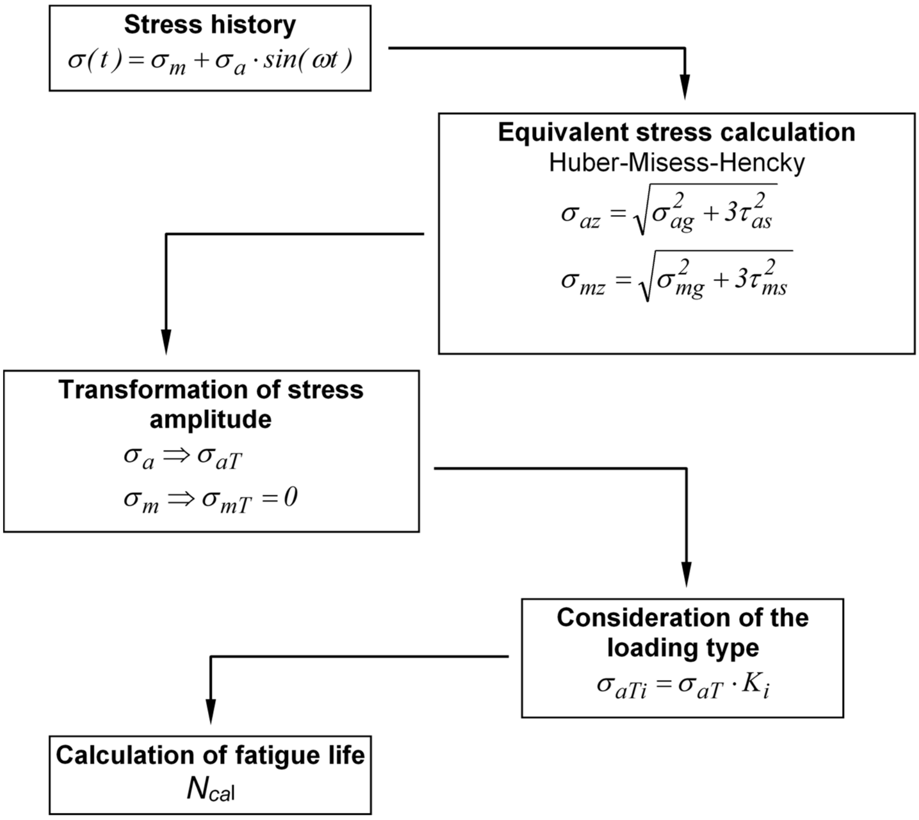

Figure 1. Algorithm for calculating fatigue life.

Where

$$\sigma_{ag} = \frac{M_a}{W_x}\cos\alpha; \quad \sigma_{mg} = \frac{M_m}{W_x}\cos\alpha,$$
$$\tau_{as} = \frac{M_a}{W_0}\sin\alpha; \quad \tau_{ms} = \frac{M_m}{W_0}\sin\alpha,$$

where: σ_{ag}, σ_{mg}—bending stress amplitude and stress mean value respectively, τ_{as}, τ_{ms}—torsional stress amplitude and stress mean value respectively, M_a, M_m—amplitude of the moment and mean value of the load moment, respectively, W_x—bending indicator, W_0—torsion indicator, α—angle between bending and torsion moments.

When transforming stress amplitudes, due to the non-zero mean stress values, commonly known transformation relationships were used. These are equations [13–15]

$$\text{Goodman}: \quad \sigma_{aT} = \frac{\sigma_a}{1-\frac{\sigma_m}{R_m}}, \tag{1}$$

$$\text{Gerber}: \quad \sigma_{aT} = \frac{\sigma_a}{1-\left(\frac{\sigma_m}{R_m}\right)^2}, \tag{2}$$

$$\text{Marin}: \quad \sigma_{aT} = \frac{\sigma_a}{\sqrt{1-\left(\frac{\sigma_m}{R_m}\right)^2}}, \tag{3}$$

where R_m—ultimate strength, σ_m—mean stress, σ_a—stress cycle amplitude with a mean value $\sigma_m \neq 0$, σ_{aT}—fatigue equivalent stress cycle amplitude (about mean value $\sigma_{mT} = 0$).

In the next transformation dependencies used in the calculations, material constants characterizing the fatigue properties of the material are used. These are the relationships [16–18]

$$\text{Morrow}: \quad \sigma_{aT} = \frac{\sigma_a}{1-\frac{\sigma_m}{\sigma'_f}}, \tag{4}$$

$$\text{Kliman}: \quad \sigma_{aT} = \frac{\sigma_a}{\left(1-\frac{\sigma_m}{\sigma'_f}\right)^{\frac{c+1}{b+c+1}}}, \tag{5}$$

where σ'_f—fatigue strength coefficient, b, c—fatigue strength and ductility exponent, respectively.

Material sensitivity to the effect of average load can be described by the material sensitivity factor for the asymmetry of cycle [2,19]. As a result of developing and transforming dependencies based on the mean loading value on Haigh diagram $\sigma_a = f(\sigma_m)$ and $\tau_a = f(\tau_m)$, their limit for stress level corresponding to the unlimited life (fatigue limit) is indicated. It was indicated that material sensitivity on mean loading is not a material constant and depends on the number of the cycles corresponding to the failure of an element. The amplitude of the corresponding normal and shear stress components is calculated as follows:

$$\sigma_a = \sigma_{-1} - \psi_\sigma \sigma_m, \tag{6}$$

$$\tau_a = \tau_{-1} - \psi_\tau \tau_m \tag{7}$$

where σ_{-1}—fatigue strength and ductility exponent, respectively fatigue limit at the oscillatory cycle, ψ_σ, ψ_τ—material sensitivity factor for the asymmetry of cycle.

The material sensitivity factor for the asymmetry of cycle ψ_σ for bending is defined as

$$\psi_\sigma = \frac{2\sigma_{-1} - \sigma_0}{\sigma_0}, \tag{8}$$

and for torsion

$$\psi_\tau = \frac{2\tau_{-1} - \tau_0}{\tau_0}, \tag{9}$$

where σ_0, τ_0—fatigue limit at one-sided cycle for bending and torsion.

The value of the factor ψ_σ and ψ_τ determined by the relationships (8) and (9) is correct for the fatigue limit. Determining the function of changing the value of the material sensitivity factor for the asymmetry of cycle depending on the number of cycles N allows the assessment of the effect of the mean stress value depending on the material life. By making the factor ψ_σ and ψ_τ dependent on the number of cycles until failure N, in Formulas (8) and (9), stress amplitudes will appear depending on the number of cycles:

for bending

$$\psi_\sigma(N) = \frac{2\sigma_{-1}(N) - \sigma_0(N)}{\sigma_0(N)}, \tag{10}$$

and for torsion

$$\psi_\tau(N) = \frac{2\tau_{-1}(N) - \tau_0(N)}{\tau_0(N)}, \tag{11}$$

where $\sigma_{-1}(N)$, $\tau_{-1}(N)$—stress amplitude at oscillatory bending and torsion for a fixed number of N cycles, $\sigma_0(N)$, $\tau_0(N)$—one-sided cycle stress amplitude under bending and torsion for a fixed number of N cycles.

After transformation Formulas (6), (7) and taking into account Relationships (10) and (11), it is possible to determine the equivalent stress amplitude at a symmetrical cycle for given values of stress amplitude σ_a and τ_a and mean values of stress σ_m and τ_m with the assumed number of cycles N

$$\sigma_{-1}(N) = \sigma_a + \psi_\sigma(N)\sigma_m, \tag{12}$$

$$\tau_{-1}(N) = \tau_a + \psi_\tau(N)\tau_m, \tag{13}$$

Assuming the stress amplitude for the symmetrical cycle, determined in accordance with the relationship (12) and (13), as the transformed amplitude and transforming the relationship (12), (13) the model based on cycle asymmetry sensitivity factor (CASF model) may be written as:

$$\sigma_{aT} = \sigma_{-1}(N) = \sigma_a\left(1 + \psi_\sigma(N)\frac{1+R}{1-R}\right), \tag{14}$$

$$\tau_{aT} = \tau_{-1}(N) = \tau_a\left(1 + \psi_\tau(N)\frac{1+R}{1-R}\right), \tag{15}$$

The proposed criterion (13) and (14) allows to determine the equivalent stress amplitude in a symmetrical cycle ($R = -1$) for the given amplitude values and the average stress value of the asymmetrical cycle ($R \neq -1$) using the function of changing the material sensitivity factor for the asymmetry of cycle.

Relations (6) to (15) have been developed for uniaxial loads and cannot be directly used for multiaxial loads, when there is also uneven stress distribution in the tested specimens.

In this paper, it is assumed that the parameters describing the Wöhler curve in the area of limited fatigue life for uniaxial loads and for the analyzed complex load cases are similar to each other, i.e., the graphs are parallel. Therefore, a constant K_i coefficient is adopted, which allows to refer the case of multiaxial loads to uniaxial tension-compression

$$K_i = \frac{Z_{rc}}{Z_i}, \tag{16}$$

where Z_{rc}—fatigue limit under cyclic tension-compression, Z_i—fatigue limit expressed by the equivalent stress amplitude for bending, torsion or a combination of bending and torsion for zero mean load, determined using the Huber-Misess-Hencky hypothesis.

Equations (1)–(6) and (15) were modified to form

$$\sigma_{aTi} = \sigma_{aT}\, K_i, \tag{17}$$

Computational fatigue life was determined from the relationship

$$log\, N_{cal} = B + A\, log\, \sigma_{aTi}, \tag{18}$$

where A, B—regression coefficients of the fatigue characteristics of the material determined at symmetrical tensile-compression.

3. Material and Methods

The smooth specimens of S355J0 steel were subjected to fatigue testing (Figure 2). The starting material was a drawn rod. The chemical composition of the material (obtained from the certificate attached to the material) is presented in Table 1. Static and fatigue properties obtained under cyclic tensile-compression are given in Table 2.

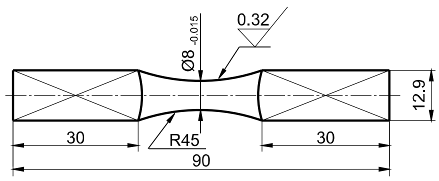

Figure 2. Shape and dimensions of specimens, dimensions in mm.

Table 1. Chemical composition of experimental material (%).

C	Mn	Si	P	S	Cr	Ni	Cu	Fe
0.21	1.46	0.42	0.019	0.046	0.09	0.04	0.17	Bal.

Table 2. Static and fatigue properties of the material.

R_e, MPa	R_m, MPa	A_{10}, %	Z, %	E, GPa	v	σ'_f, MPa	b	c	n'	K' MPa
357	535	21	50	210	0.30	782	−0.118	−0.410	0.287	869

The tests were carried out on the fatigue test stand MZGS-100 [20,21]. The stand used in experiment allows to perform cyclic of bending, torsion and both combined. The tests of cyclic bending and torsion were conducted within the range of low and high number of cycles with controlled force (in the considered case, the moment amplitude was controlled). The loads were of a sinusoidal nature with a frequency of about 25–29 Hz. The amplitudes and the mean value of the load were changed according to the test requirements. The nominal stress amplitude and nominal mean stress value were used in calculations.

The tests included three load states of the samples determined by the angle α determining the combination of bending and torsion (Figure 3). It is easy to find, that for $\alpha = 0$ we have $M_{g\alpha}(t) = M(t)$—the specimen is subjected to bending. When $\alpha = 90°$, we have $M_{g\alpha}(t) = M(t)$—the specimen is subjected to torsion. The combined bending with torsion is applied to specimen for every value of the angle in range $0 < \alpha < 90°$. For combined bending with torsion, torsion moment $M_{g\alpha}(t)$ is proportional to bending moment $M_{g\alpha}(t)$, where proportion is equal to tgα.

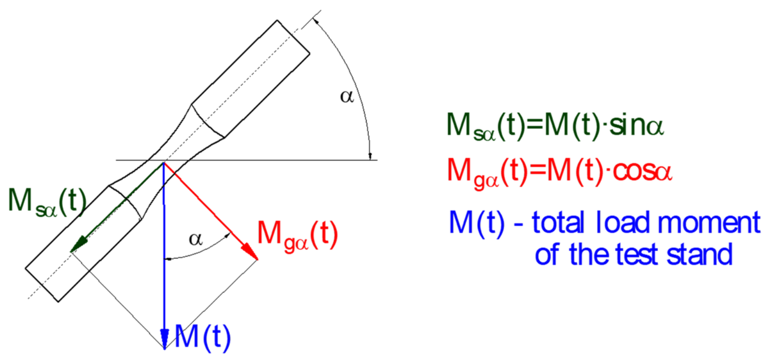

Figure 3. The load scheme of the fatigue test stand MZGS 100.

For test three values of the angle α were used:

α = 0 (rad), (0°) (bending),
α = 1.107 (rad), (63.5°) (combined bending with torsion),
$M_{s\alpha} = 2M_{g\alpha};\ \sigma_\alpha(t) = \tau_\alpha(t)$,
α = π/2 (rad), (90°) (torsion).

Experimental studies were conducted at a constant value of the stress ratio R = −1, −0.5, 0 by changing the moment amplitude value M_{ag} and the mean moment value M_{mg} for bending and M_{as} and M_{ms} respectively for torsion. The tests were performed for 4–5 levels of stress amplitudes, for each combination of load at least two or three specimens were used. As a result, for the given load levels, the corresponding fatigue life was obtained. Obtaining fracture of specimen was adopted as the failure criterion for the sample.

Standard fatigue characteristics for cyclic tension–compression are described by equation [22]

$$log\, N_{cal} = B + A\, log\, \sigma_a = 24.32 - 7.91 log\sigma_a, \tag{19}$$

where the limits of confidence intervals with a probability of 0.95 for individual parameters are as follows: $-6.16 \leq A \leq$ n − 9.67; $20.04 \leq B \leq 28.60$. The fatigue limit obtained is Z_{rc} = 204 MPa and correspond her $N_0 = 1.12 \times 10^6$ cycles.

4. Results and Discussion

The results of bending fatigue tests were approximated by the regression equation in the form (in the case of torsion, the equation contains τ_a)

$$log\, N_{\exp} = B + A log\sigma_a, \tag{20}$$

Figure 4 show the results of tests on bending, torsion and combination of bending with torsion as well as fatigue characteristics determined based on Equation (20).

Table 3 contains the values of the parameters of the regression equation and the correlation coefficient r values of log$N$ and logσ_a (logτ_a), while Table 4 contains the fatigue limits for individual load combinations.

Table 3. Parameters of the regression equation.

R	Bending			Torsion			Bending and Torsion		
	B	*A*	*r*	*B*	*A*	*r*	*B*	*A*	*r*
−1	23.93	−7.19	−0.97	32.81	−11.82	−0.94	29.73	−10.62	−0.98
−0.5	23.71	−7.40	−0.96	27.60	−10.01	−0.93	36.73	−14.67	−0.99
0	31.40	−10.73	−0.96	59.76	−25.25	−0.95	31.62	−12.42	−0.94

Table 4. Fatigue limits.

Moment and Stress	Bending	Bending and Torsion	Torsion
	α = 0°	α = 63.5°	α = 90°
M_a (N·m)	13.59	16.82	17.53
σ_{-1} (τ_{-1}) (MPa)	σ_{-1} = 271	$\sigma_{-1} = \tau_{-1}$ = 152	τ_{-1} = 175

Analyzing the graphs in Figure 4 and the parameters contained in Table 3, it can be concluded that the values of the coefficient A for bending are similar in all cases except R = 0 (A = −10.73). During torsion for R = −1 and −0.5, the values of coefficient A are close to each other, while for R = 0 its value clearly differs from the others. In the case of a combination bending with torsion, the values of the coefficient A are similar for R from −1 to 0.

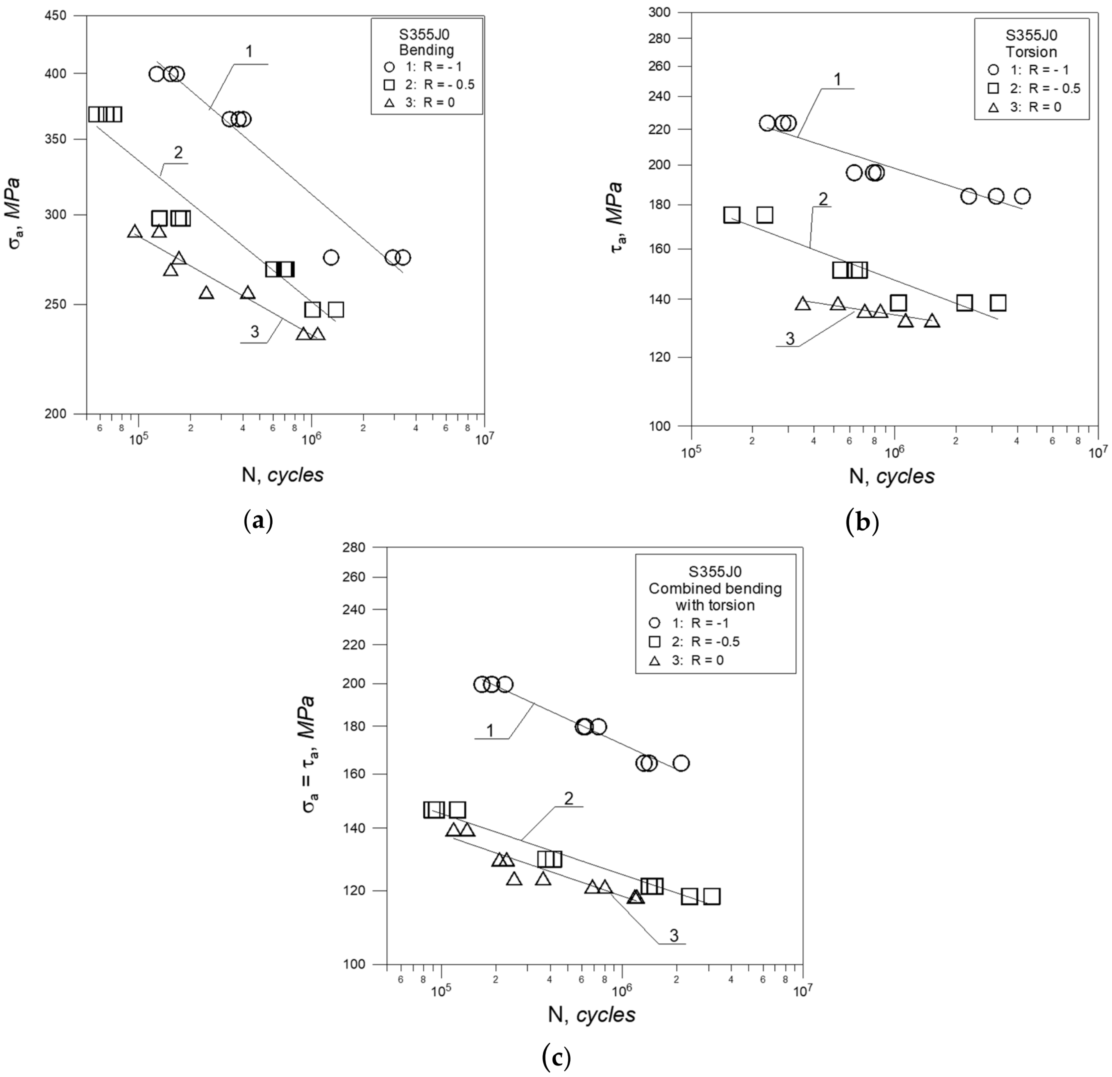

Figure 4. The results of fatigue tests on: (**a**) bending, (**b**) torsion, (**c**) bending with torsion.

Increasing the value of the stress ratio R from −1 to 0 causes a significant decrease in the permissible (acceptable) amplitudes. In the case of bending, R = −0.5 allowable amplitudes are about 20% lower than for $R = -1$ (at $\sigma_m = 0$) and for $R = 0$ they are 35% lower. During torsion for $R = -0.5$, the allowable stress amplitudes are about 19% smaller compared to the stress amplitudes for $R = -1$, while for $R = 0$ this decrease is from 40% for a small number of cycles and up to 27% for a large number of cycles. For the combination bending with torsion under $R = -0.5$ the stress amplitudes are reduced by 35% for a small number of cycles and to 27% for a large number of cycles, while for $R = 0$ the allowable stress amplitudes are reduced for a small and a large number of cycles respectively 37% and 32%.

Figure 5 show the impact of the mean value of bending stress σ_m and torsional stress τ_m on the change in allowable stress amplitudes σ_a and τ_a. Lines in Figure 5 present the interpolation of the data on the graph.

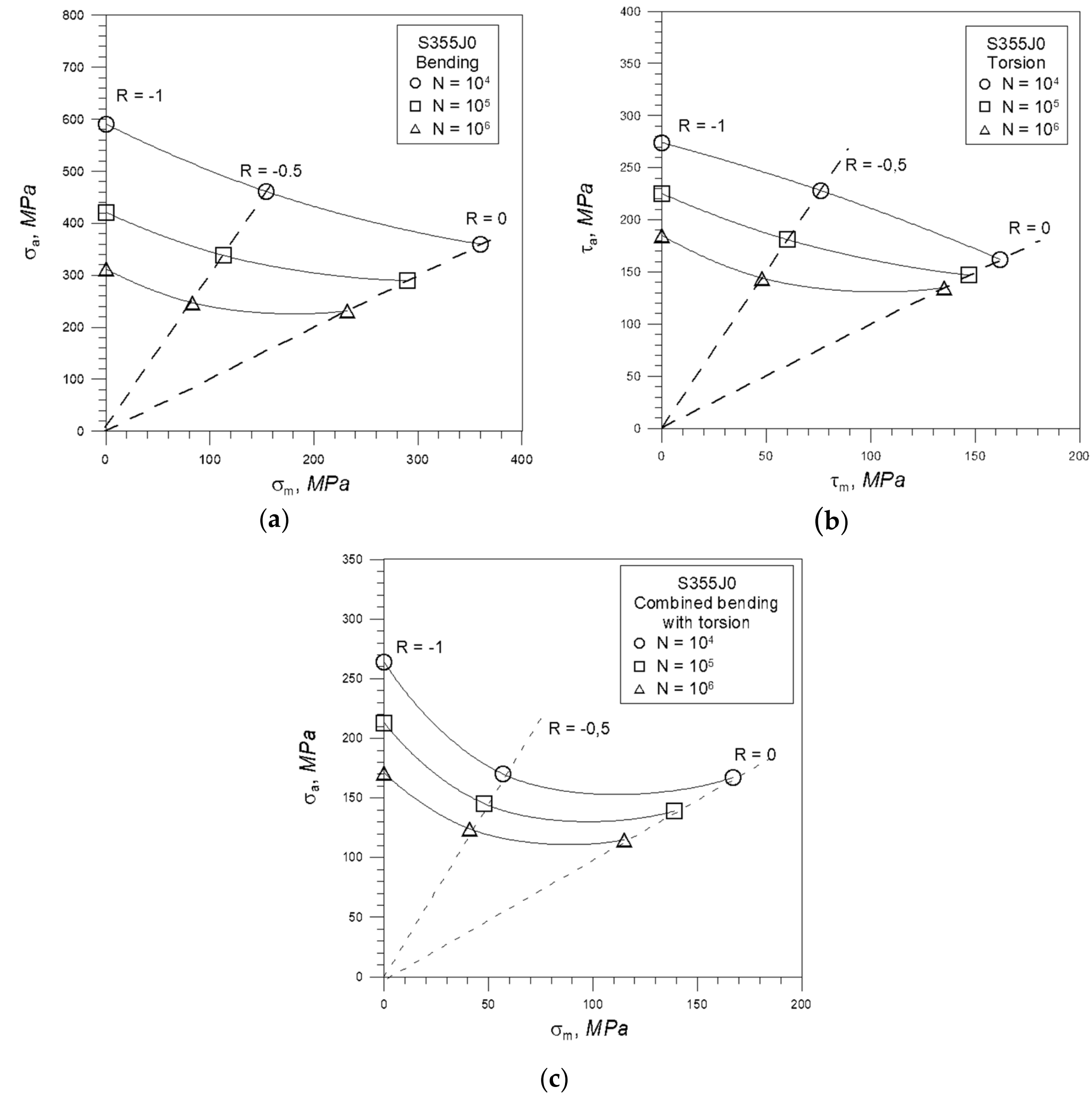

Figure 5. The dependence of the stress amplitude on the mean stress for: (**a**) bending, (**b**) torsion, (**c**) bending with torsion.

In the case of bending (Figure 5a) for a lifetime of 10^4 cycles, an increase in the mean stress value σ_m in relation to $\sigma_m = 0$ causes a decrease in the stress amplitude σ_a to varying degrees, e.g., for $R = 0.5$ by 22% and for $R = 0$ by 39%. For durability $N = 10^5$ cycles, the decreases in σ_a are 20% and 30% for $R = -0.5$ and 0, respectively. These differences for all R values are no longer as large as for $N = 10^4$ cycles. However, in the case of durability at the level of 10^6 cycles, there is a decrease in the value of stress amplitude σ_a by an average of 23% in relation to $\sigma_m = 0$, while for $R = -0.5$ and 0 the value of allowable stress amplitude practically does not depend on the value of the mean stress.

During torsion (Figure 5b), for life $N = 10^4$ cycles, a significant decrease in stress τ_a due to the increase in value τ_m is also visible, e.g., in relation to loads $\tau_m = 0$ the decrease is 17% and for $R = -0.5$ and about 40% for $R = 0$. At durability level $N = 10^5$ cycles these decreases are 20% and 34% respectively. For a large number of cycles, this difference virtually disappears and the decrease in the permissible amplitude values is very similar (23% and 27%).

For the combination of bending with torsion (Figure 5c) and durability $N = 10^4$ cycles, it can be seen that with an increase in average stress, there is a large decrease in the allowable stress amplitudes (about 35%) for both $R = -0.5$ and $R = 0$. Similarly, for $N = 10^5$ cycles- the decrease in the allowable stress amplitudes are 31% and 34% for $R = -0.5$ and $R = 0$, respectively. For $N = 10^6$ cycles, an increase in the mean stress value reduces the stress amplitude by 32% for $R = -0.5$ and 27% for $R = 0$ compared to the case $\sigma_m = \tau_m = 0$. The small influence of the mean stress value from the durability level $N = 10^5$ cycles is characteristic. A further increase in mean stress practically does not cause major changes in the values of allowable stress amplitudes.

Using the relationships (10) and (11) on the basis of fatigue tests, the value of the ψ coefficient was determined in terms of life $N = (5{\cdot}\times 10^4 - 2.5 \times 10^6)$ cycles. The change of the value of the factor ψ depending on the number of cycles N is shown in Figure 6. For bending, this relationship was described by the function $\psi_\sigma(N) = 3.1621N^{-0.164}$. There is a visible decrease in the value of the factor in terms of durability $N = (5{\cdot}\times 10^4 - 7.5{\cdot}\times 10^5)$ cycles. In the case of torsion, the function has the form $\psi_\tau(N) = 2.897\mathrm{N}^{-0.131}$, while the nature of the curve is similar to that for bending. In the case of a combination of bending and torsion, the function takes the form $\psi_\tau(N) = \psi_\sigma(N) = 0.854\mathrm{N}^{-0.044}$. From this function one can notice a milder course than for bending and torsion, with the largest decreases in the coefficient value also occurring in the durability range $N = (5{\cdot}\times 10^4 - 7.5{\cdot}\times 10^5)$ cycles.

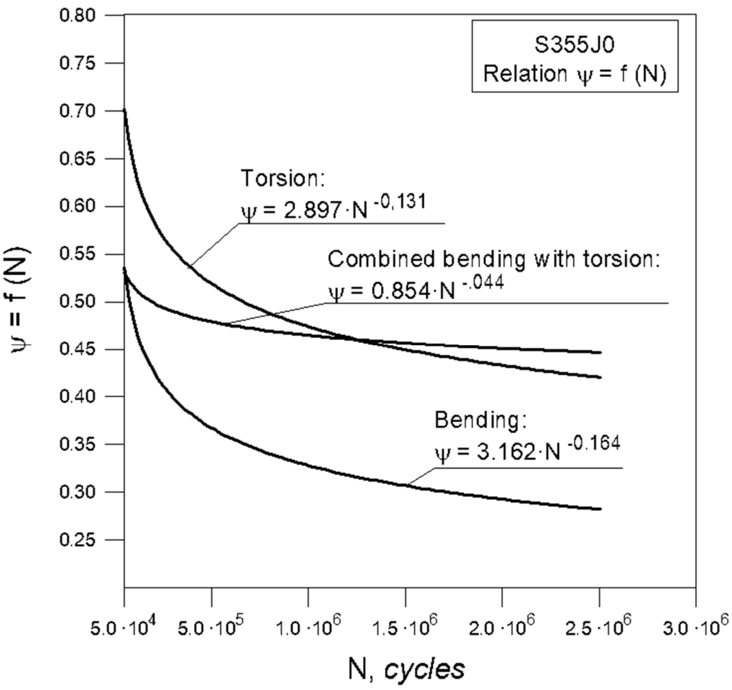

Figure 6. Change of the material sensitivity factor $\psi = f(N)$ for the asymmetry of cycle.

In the algorithm of calculating fatigue life for bending, torsion and combination of bending with torsion with the participation of mean stress values, the transformation relationships described by Equations (1)–(5) and (14), (15) modified to form (17), were used.

The values of K_i (16) coefficients were determined assuming the fatigue limits of individual types of loads at $\sigma_m = \tau_m = 0$ (Table 4) respectively:

for bending

$$K_g = \frac{Z_{rc}}{\sigma_{-1}};\ \sigma{-1} = 271\ \mathrm{MPa}, \tag{21}$$

for torsion

$$K_s = \frac{Z_{rc}}{\sqrt{3}{\cdot}\tau_{-1}};\ \tau{-1} = 152\ \mathrm{MPa}, \tag{22}$$

for bending and torsion

$$K_{gs} = \frac{Z_{rc}}{\sqrt{\sigma_{-1}^2 + 3\cdot\tau_{-1}^2}};\ \sigma{-1} = \tau{-1} = 175\ \mathrm{MPa}. \tag{23}$$

Stress amplitudes σ_{aTi} were determined from Equation (17), computational stability N_{cal} according to Equation (18), which is the fatigue characteristics of the tested steel under uniaxial tension-compression (where there is an even distribution of stress across the specimen cross-section).

Figure 7 shows the results of calculations for bending, torsion and a combination of bending and torsion with zero mean value of the load course. Figures 8–10 show a comparison of the design fatigue life with the experimentally obtained life for bending, torsion and combination of bending and torsion for non-zero mean stress values. The solid line means the perfect match between the computational stability N_{cal} and the experimental N_{exp}, while the dashed lines represent the scatter bands of results with the coefficients N_{cal}/N_{exp} = 3 (1/3).

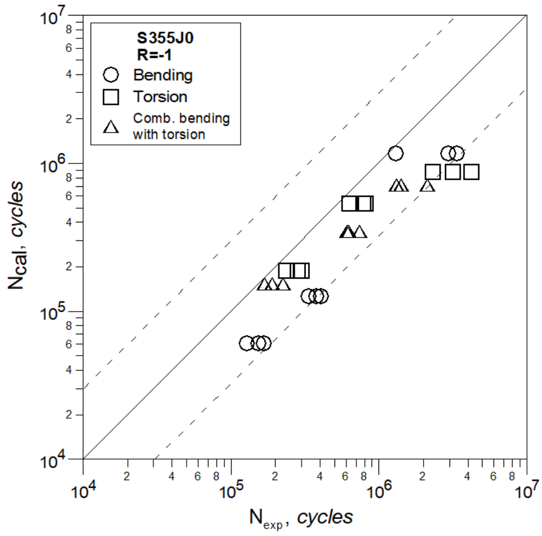

Figure 7. Comparison of the computational life N_{cal} with the experimental N_{exp} for R = −1.

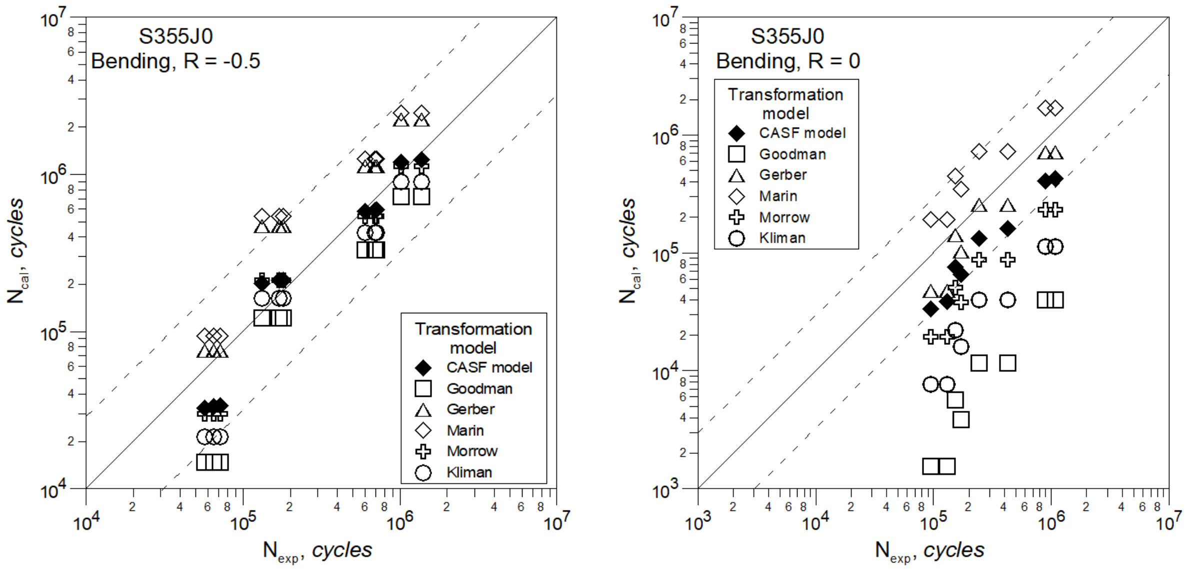

(**a**) (**b**)

Figure 8. Comparison of the computational life N_{cal} with the experimental N_{exp} under bending for: (**a**) R = −0.5, (**b**) R = −0.

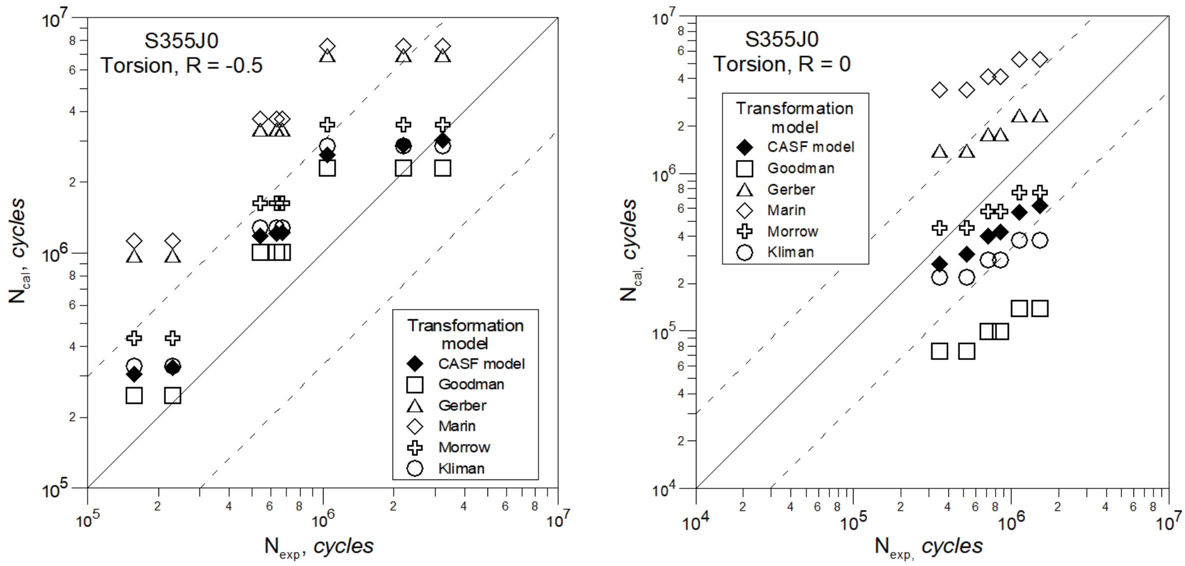

(**a**) (**b**)

Figure 9. Comparison of the computational life N_{cal} with the experimental N_{exp} under torsion for: (**a**) $R = -0.5$, (**b**) $R = -0$.

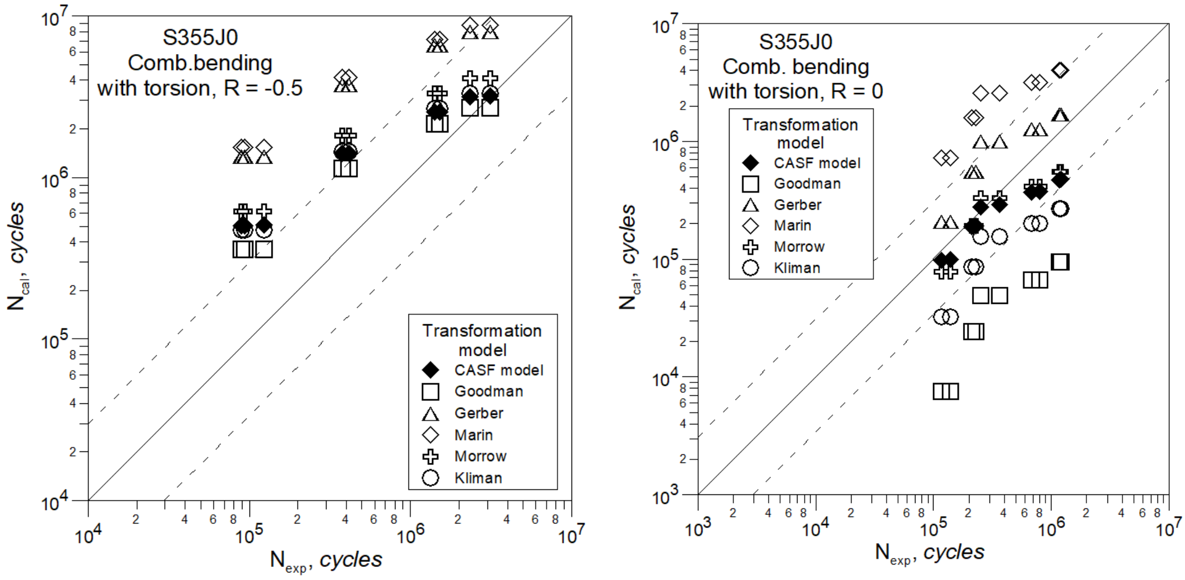

(**a**) (**b**)

Figure 10. Comparison of the computational life N_{cal} with the experimental N_{exp} under bending and torsion for: (**a**) $R = -0.5$, (**b**) $R = -0$.

Figure 7 shows that the computational life are mostly in the result spread band regardless of the type of load and its value. The exception is torsion for a large number of cycles. This allows to state that the assumption adopted in Formula (16) gives satisfactory results of calculations for zero-mean loads and allows to believe that it will be used for other load cases.

The analysis of Figure 8a shows that in the case of bending for $R = -0.5$, the best agreement was obtained thanks to the Morrow transform dependence and the model described by Equation (14). Satisfactory results were also obtained for the remaining relationships. However, their dispersion is greater than for the previously indicated.

At bending loads for $R = 0$ (Figure 8b), correct results of fatigue life calculations were obtained using Gerber, Marin and CASF model (Equation (14)). The calculation results are in the scatter band with the $N_{cal}/N_{exp} = 3$ (1/3) coefficient for all three cases. It should be noted, however, that this model underestimates computational durability compared to experimental. The remaining transformation formulas clearly underestimate the calculated fatigue life; the calculation results are outside the scatter band $N_{cal}/N_{exp} = 3$ (1/3).

Figure 9 shows the results of calculations for torsion. In the case of $R = -0.5$ (Figure 9a), the best results are obtained by the relationship between Goodman and Kliman and the calculation of fatigue life using Equation (15), satisfactory results were obtained for the Morrow relationship. Gerber and Marina's transformation dependencies significantly overstate the results of calculations compared to the results obtained experimentally. For the stress ratio $R = 0$ cycle (Figure 9b), the best results of fatigue life calculations were obtained for Morrow's formula and calculated according to Equation (15).

In the case of a combination of bending and torsion for $R = 0.5$ (Figure 10), the best results of fatigue life assessment were obtained for Goodman and Kliman relationships. Calculations using Equation (14) overstate the computational life for a small number of cycles. For $R = 0$ when bending with torsion (Figure 10b), the best compatibility is given by the assessment of durability using the model defined by Equation (14) and the Morrow and Gerber relationships.

5. Conclusions

The following conclusions can be drawn from the tests performed on S355J0 steel specimens at proportional bending with torsion loads for different values of the R:

1. In the case when $R = -1$ satisfactory results of the fatigue life assessment for bending, torsion and a combination of bending and torsion were obtained using the K_i coefficient, which is the ratio of the fatigue limit at cyclic tension-compression to the fatigue limit, calculated in accordance with the Huber–Misess–Hencky hypothesis for analyzed loads.
2. For loads with a non-zero mean value, it was found that:
    - satisfactory results of the fatigue life assessment for bending were obtained using the Gerber transformation dependence and the CASF model described by Equation (14),
    - in the case of torsion, the best compatibility of computational fatigue life with experimental life is obtained by using Equation (15) and Morrow's formula,
    - for the combination of bending and torsion for both $R = -0.5$ and $R = 0$, the CASF model gives the best results of fatigue life assessment.
3. The CASF model described by Equations (14) and (15), including the effect of the mean stress value on fatigue life using the material sensitivity factor for the asymmetry of cycle, gives good results for predicting fatigue life for all tested load cases.

Author Contributions: Conceptualization, R.P.; formal analysis, R.P., D.R.; investigation, R.P.; methodology, R.P.; writing–original draft, R.P., D.R. All authors have read and agreed to the published version of the manuscript.

Funding: This research received no external funding.

Conflicts of Interest: The authors declare no conflict of interest.

References

1. Wehner, T.; Fatemi, A. Effect of mean stress on fatigue behavior of a hardened carbon steel. *Int. J. Fatigue* **1991**, *13*, 241–248. [CrossRef]
2. Gołoś, K.M.; Eshtewi, S.H. Multiaxial Fatigue and Mean Stress Effect of St5 Medium Carbon Steel. In Proceedings of the 5th International Conference on Biaxial/Multiaxial Fatigue and Fracture, Cracow, Poland, 8–12 September 1997; Volume 1, pp. 25–34.
3. Glinka, G.; Shen, G.; Plumtree, A. Mean stress effect in multiaxial fatigue. *Fatigue Fract. Eng. Mater. Struct.* **1995**, *18*, 755–764. [CrossRef]

4. Skibicki, D.; Sempruch, J.; Pejkowski, L. Model of non-proportional fatigue load in the form of block load spectrum. *Mater. Sci. Eng. Techonl.* **2014**, *45*, 68–78. [CrossRef]
5. Liu, Y.; Mahadevan, S. Multiaxial high-cycle fatigue criterion and life prediction for metals. *Int. J. Fatigue* **2005**, *27*, 790–800. [CrossRef]
6. Kluger, K.; Pawliczek, R. Assessment of validity of selected criteria of fatigue life prediction. *Materials* **2019**, *12*, 2310. [CrossRef] [PubMed]
7. Rozumek, D.; Marciniak, Z. Fatigue properties of notched specimens made of FeP04 steel. *Mater. Sci.* **2012**, *47*, 462–629. [CrossRef]
8. Prażmowski, M.; Rozumek, D.; Paul, H. Static and fatigue tests of bimetal Zr-steel made by explosive welding. *Eng. Fail. Anal.* **2017**, *75*, 71–81. [CrossRef]
9. Branco, R.; Costa, J.D.; Berto, F.; Antunes, F.V. Effect of loading orientation on fatigue behaviour in severely notched round bars under non-zero mean stress bending-torsion. *Theor. Appl. Fract. Mech.* **2017**, *92*, 185–197. [CrossRef]
10. Carpinteri, A.; Kurek, M.; Łagoda, T.; Vantadori, S. Estimation of fatigue life under multiaxial loading by varying the critical plane orientation. *Int. J. Fatigue* **2017**, *100*, 512–520. [CrossRef]
11. Rozumek, D.; Faszynka, S. Influence of the notch radius on fatigue crack propagation in beam specimens of 2017A-T4 alloy. *Mater Sci.* **2017**, *53*, 417–423. [CrossRef]
12. Vicente, C.M.S.; Sardinha, M.; Reis, L. Failure analysis of a coupled shaft from a shredder. *Eng. Fail. Anal.* **2019**, *103*, 384–391. [CrossRef]
13. Marin, J. Interpretation of fatigue strengths for combined stresses. In Proceedings of the International Conference on Fatigue of Metals, London, UK, 10–14 September 1956; pp. 184–194.
14. Goodman, J. *Mechanics Applied to Engineering*, 9th ed.; Longmans, Green and Co.: New York, NY, USA, 1954.
15. Gerber, W. Determination of permissible stresses in iron constructions. *Zeitschrift des Bayerischen Architekten- und Ingenieur-Vereins* **1974**, *6*, 101–110. (In German)
16. Pawliczek, R.; Kluger, K. Influence of irregularity coefficient of loading on calculated fatigue life. *J. Theor. Appl. Mech. Lett.* **2013**, *51*, 4.
17. Morrow, J. *Fatigue Design Handbook, Advances in Engineering*; Society of Automotive Engineers: Warrendale, PA, USA, 1968; Volume 4, p. 29.
18. Kliman, V. Prediction of Random Load Fatigue Life Distribution. In *Fatigue Design, ESIS 16*; Mechanical Engineering Publications: London, UK, 1993; pp. 241–255.
19. Kocańda, S.; Szala, J. *Basics of Fatigue Calculations*; PWN: Warsaw, Poland, 1997. (In Polish)
20. Achtelik, H.; Kurek, M.; Kurek, A.; Kluger, K.; Pawliczek, R.; Łagoda, T. Non-standard fatigue stands for material testing under bending and torsion loadings. *AIP Conf. Proc.* **2018**, *2029*, 020001.
21. Rozumek, D.; Marciniak, Z.; Lachowicz, C.T. The energy approach in the calculation of fatigue lives under non-proportional bending with torsion. *Int. J. Fatigue* **2010**, *32*, 1343–1350. [CrossRef]
22. ASTM E 739-80: Standard practice for statistical analysis of linearized stress-life (S-N) and strain-life (-N) fatigue data. In *Annual Book of ASTM Standards*; ASTM International: Philadelphia, PA, USA, 1989; Volume 03.01, pp. 667–673.